esa

→ EARTH OBSERVATION SUMMER SCHOOL

Earth System Monitoring & Modelling

30 July–10 August 2018 | ESA–ESRIN | Frascati (Rome) Italy

OCEAN CIRCULATION

Marie-Hélène RIO

OCEAN CIRCULATION

Wednesday: Introduction

- ❑ The different components of the ocean circulation
- ❑ How to estimate (part of) the ocean circulation
  - ✓ from oceanographic in-situ measurements
  - ✓ from space

Thursday: Space and in-situ data synergy for a better retrieval of the ocean circulation

- ❑ Altimetry, geoid, drifters, hydrological profiles for estimating the ocean mean circulation
- ❑ Altimetry, drifters, scatterometers for estimating the Ekman currents
- ❑ SSH/SST synergy for higher resolution surface currents

Friday: The 3D perspective

- ❑ The thermohaline circulation
- ❑ Reconstruction of the 3D horizontal ocean circulation from observations
- ❑ Estimation of the vertical velocity component

The surface of an ocean of homogeneous density covering an Earth at rest would coincidate with an Earth Gravity Equipotential surface called GEOID

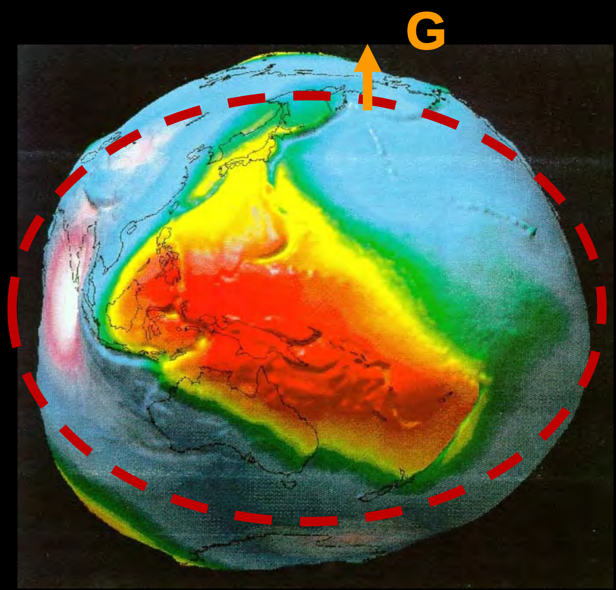

E : Reference Ellipsoid

Equipotential of the gravity field

The surface of an ocean of homogeneous density covering an Earth at rest would coincidate with an Earth Gravity Equipotential surface called GEOID

Gravity forces generating tides

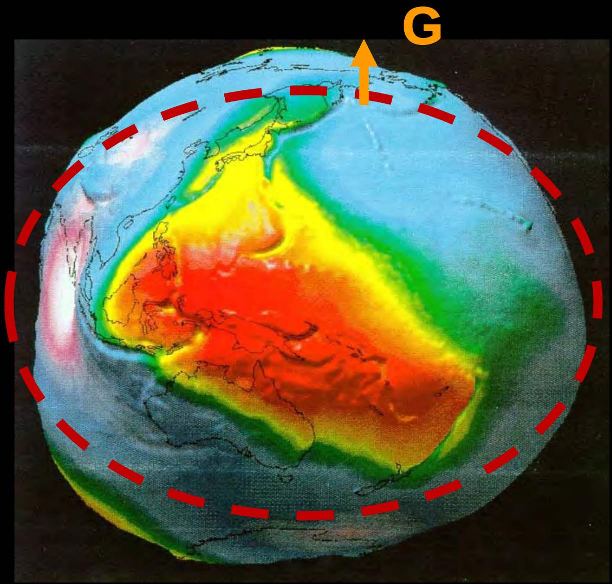

Thermal forcing

Variations of the Atmospheric pressure

Wind effects

Hydrological Cycle

Coriolis Force due to the Earth Rotation

As a consequence, at a given time, at a given place, the sea level differs from its position at rest, the geoid. The difference between the two positions is the **ocean dynamic topography h**

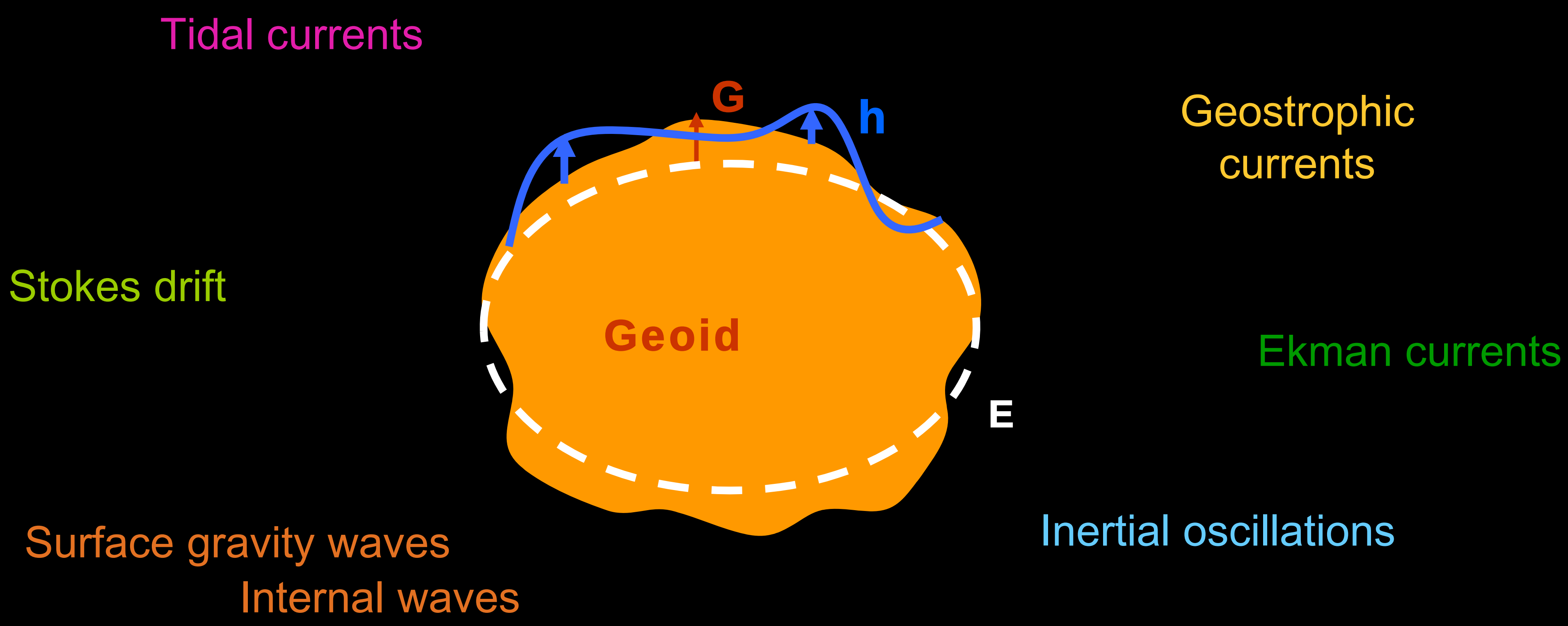

The equation of motion

$$\frac{D\vec{u}}{Dt} = -2\vec{\Omega} \wedge \vec{u} - \frac{1}{\rho}\vec{\nabla}p - \vec{g} + \nu\vec{\nabla}^2\vec{u}$$

(1) (2) (3) (4)

The lagrangian acceleration of a fluid particule is due to 4 main forces:

(1) Coriolis force due to Earth rotation
(2) Pressure gradient force
(3) Gravitation force
(4) Friction forces

Different approximations can be done depending on the relative order of magnitude of these 4 forces

R_0=(non linear terms)/(Coriolis term) E=(friction term / Coriolis term)

The geostrophic circulation

E<10^{-3} R$_0$<10^{-3} and w<<u,v

Away from the boundary layers and away from the equator, over large (> 50-100 km) spatial and long (>2-10 days) temporal scales ocean is to the first order in geostrophic balance.

The largest terms in the equations of motion reduce to the Coriolis force and the pressure gradient.

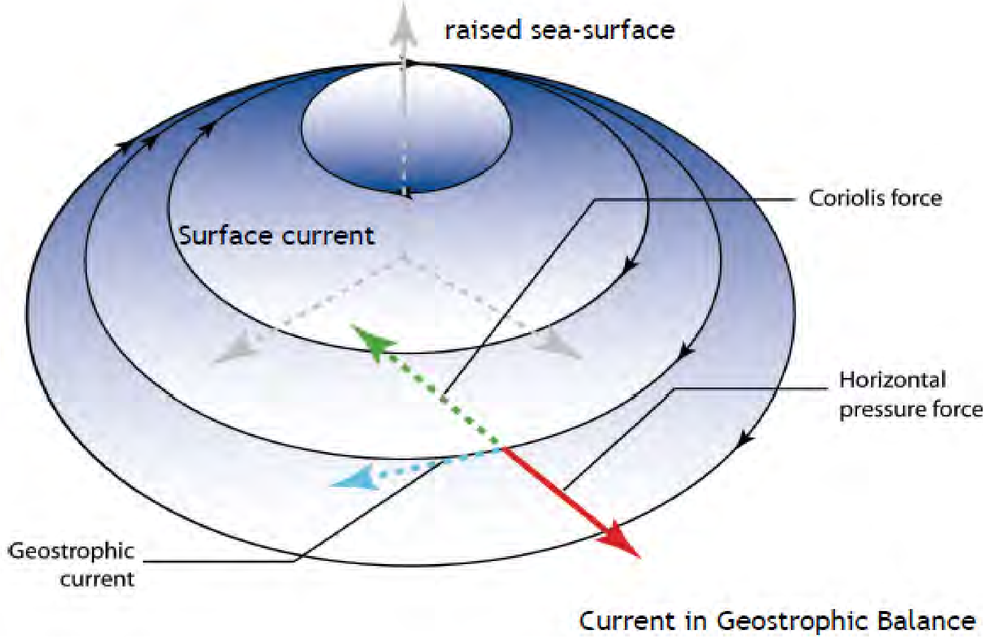

$$0 = -\frac{1}{\rho}\frac{\partial p}{\partial x} + fv$$

$$0 = -\frac{1}{\rho}\frac{\partial p}{\partial y} - fu$$

+ Hydrostatic equation

$$0 = -\frac{1}{\rho}\frac{\partial p}{\partial z} - g$$

$$u_{geo} = -\frac{g}{f}\frac{\partial h}{\partial y}$$

$$v_{geo} = \frac{g}{f}\frac{\partial h}{\partial x}$$

The ocean surface velocity field (u,v) can be readily obtained from the gradients of h, the sea level above the geoid h.

The barotropic / baroclinic circulation

E<10⁻³ R₀<10⁻³

Away from the boundary layers and away from the equator, over large (> 50-100 km) spatial and long (>2-10 days) temporal scales ocean is to the first order in geostrophic balance

The largest terms in the equations of motion reduce to the Coriolis force and the pressure gradient

$$0 = -\frac{1}{\rho}\frac{\partial p}{\partial x} + fv$$

$$0 = -\frac{1}{\rho}\frac{\partial p}{\partial y} - fu$$

+ Hydrostatic equation

$$0 = -\frac{1}{\rho}\frac{\partial p}{\partial z} - g$$

$$f\frac{\partial \vec{u}}{\partial z} = \frac{1}{\rho^2}\vec{\nabla}p \wedge \vec{\nabla}\rho$$

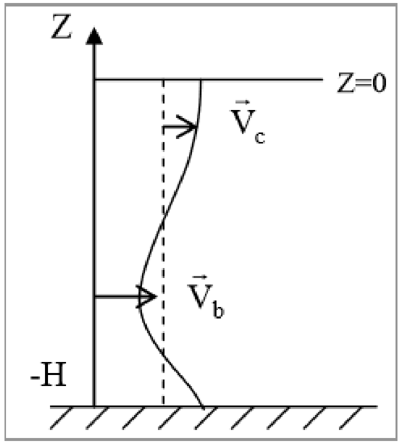

Baroctropic circulation: isobars and isopycnals are parallel. $\vec{\nabla}p \wedge \vec{\nabla}\rho = \vec{0}$

$\vec{u}$ is constant on the vertical Density is fonction of pressure only ρ=ρ(p)

Baroclinic circulation: isobars and isopycnals intersect. $\vec{u}$ is not anymore constant on the vertical. Density does not vary only with pressure but also laterally

The thermal wind equation

$E<10^{-3}$ $R_0<10^{-3}$

Away from the boundary layers and away from the equator, over large (> 50-100 km) spatial and long (>2-10 days) temporal scales ocean is to the first order in geostrophic balance

The largest terms in the equations of motion reduce to the Coriolis force and the pressure gradient

$$0 = -\frac{1}{\rho}\frac{\partial p}{\partial x} + fv$$

$$0 = -\frac{1}{\rho}\frac{\partial p}{\partial y} - fu$$

\+ *Hydrostatic equation*

$$0 = -\frac{1}{\rho}\frac{\partial p}{\partial z} - g$$

$$u_{geo}(z = z_i) = ugeo\left(z = z_{ref}\right) + \frac{g}{\rho f}\int_{z=zref}^{zi}\frac{\partial \rho}{\partial y}\rho'(z)dz$$

$$v_{geo}(z = z_i) = vgeo\left(z = z_{ref}\right) - \frac{g}{\rho f}\int_{z=zref}^{zi}\frac{\partial \rho}{\partial x}\rho'(z)dz$$

$\rho'(z) = \rho(z) - \rho_0$

Mean geostrophic currents speed
From Altimetry+GOCE+in-situ measurements

Rio et al, 2014

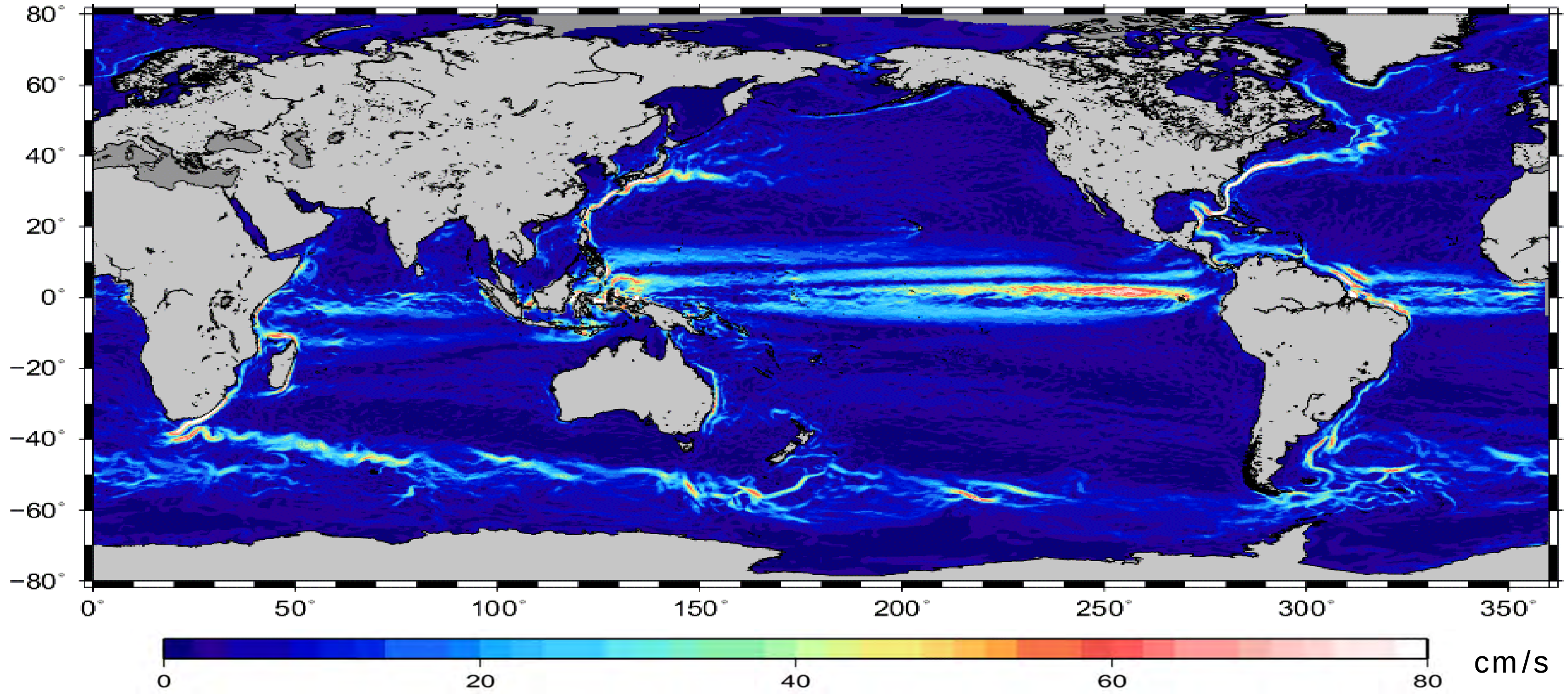

The Ekman currents

$R_0 << 1$, $E \sim 1$ In an homogenous spatial area, u, v, ω and stability conditions, under a stationary temporal forcing, τ_e over a few inertial periods, the equilibrium between the Coriolis forces and the friction forces due to wind stress leads to the classical Ekman current formulation.

$$-fv_E = A_z \frac{\partial^2 u_E}{\partial z^2} = \frac{1}{\rho} \frac{\partial \tau_x}{\partial z} \qquad fu_E = A_z \frac{\partial^2 v_E}{\partial z^2} = \frac{1}{\rho} \frac{\partial \tau_y}{\partial z}$$

$$u_e = \pm \frac{\pi\sqrt{2}}{\rho(f+w)D_e} e^{\frac{\pi}{D_e} z} * \tau_e * \cos\left(\frac{\pi}{4} + \frac{\pi}{D_e} z\right)$$

$$v_e = \frac{\pi\sqrt{2}}{\rho(f+w)D_e} e^{\frac{\pi}{D_e} z} * \tau_e * \sin\left(\frac{\pi}{4} + \frac{\pi}{D_e} z\right)$$

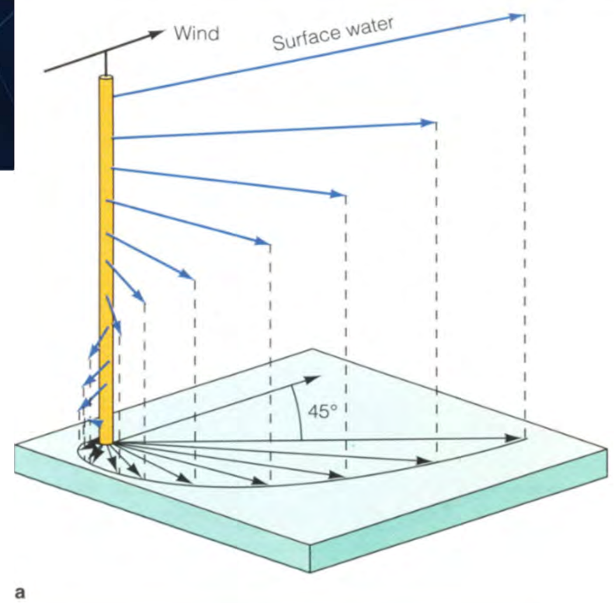

τ_e = Effective Wind Stress

D_e = Ekman depth

f = planetary vorticity

w = local vorticity

$$2\omega = \partial_x vgeost - \partial_y ugeost$$

Stokes drift

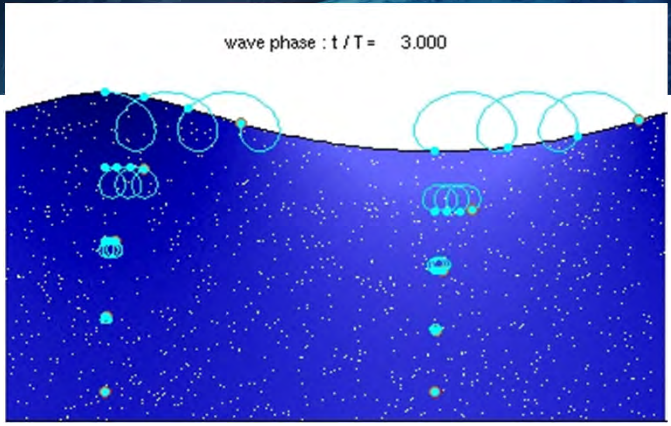

G.G. Stokes (1847) discovered that as waves travel, the water particles that make up the waves do not travel in a straight line, but rather in orbital motions.
As the particles progress in an orbital motion, their movement is enhanced at the top of the orbit and slowed slightly at the bottom.
As a consequence water particles have an additional movement in the direction of wave propagation.

$$\overline{u}_S \approx \omega k a^2 e^{2kz} = \frac{4\pi^2 a^2}{\lambda T} e^{4\pi z/\lambda}.$$

a is the wave amplitude, *k* is the wave number: $k = 2\pi / \lambda$,
ω is the angular frequency: $\omega = 2\pi / T$,
z is the vertical coordinate, with positive *z* pointing out of the fluid layer,
λ is the wave length and *T* is the wave period

$H_{sw} \approx 0.02\, U_{10}^2$ =2m in 10 m/s wind speed

Mean Stokes drift over one month (September 2009) calculated from the WW3 model

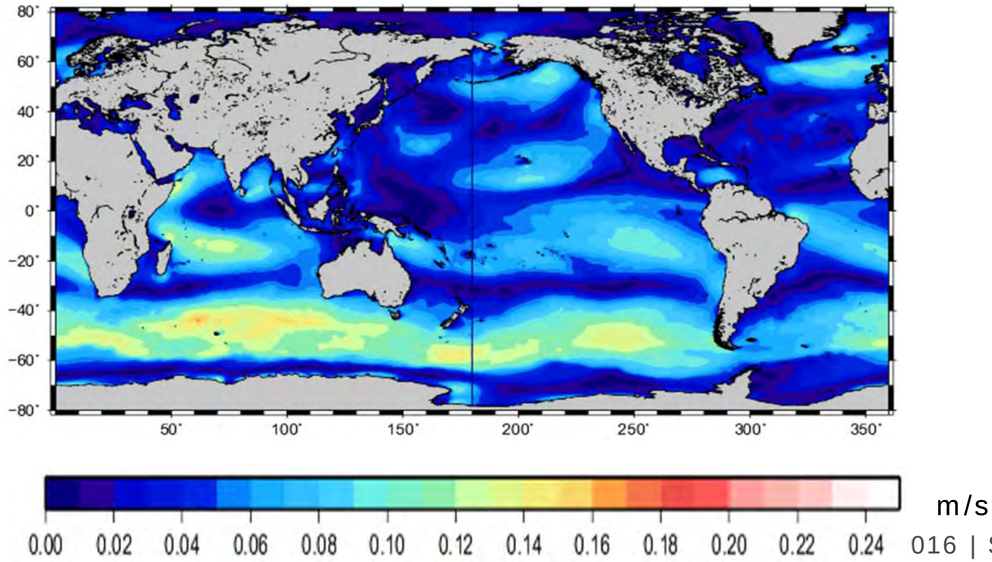

The wind driven (Ekman+Stokes) current

Near the surface, the surface Stokes drift induced by the waves typically accounts for 2/3 of the total surface wind-induced drift.

Stokes drift modifies the classical Ekman induced current spiral (from Ardhuin et al, 2009). Here, radar HF measured vector, $\boldsymbol{U_R}$*, has been interpreted as a sum of a quasi-Eulerian current,* $\boldsymbol{U_E}$*, representative of the upper 2 m and a filtered surface Stokes drift,* $\boldsymbol{U_{Sf}}$*.*

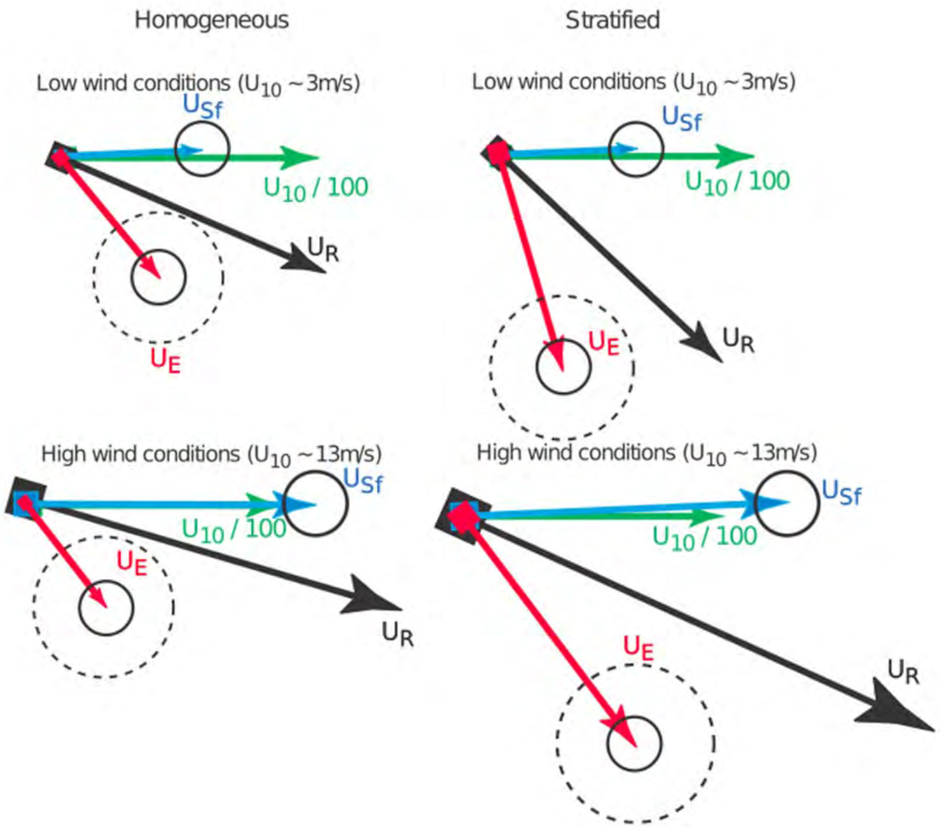

Inertial Oscillations

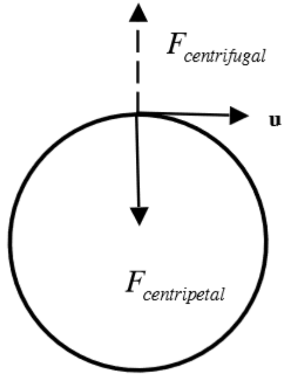

When wind and wave forces that have set upper ocean motions cease to strongly act, water will not rest immediately. Energy imparted by the wind and waves takes time to fully dissipate. The Coriolis force will then continue to apply as a **centripetal force**, leading to **rotational flows**, referred as **inertial currents**. The period of rotation will vary with the local Coriolis parameter f (e.g. latitude dependent).

$$\frac{\partial u}{\partial t} - fv = 0 \qquad \frac{\partial v}{\partial t} + fu = 0 \quad \Longrightarrow \quad \begin{array}{l} u=U\sin(ft) \\ v=U\cos(ft) \end{array}$$

Example of inertial oscillations offshore Brazil

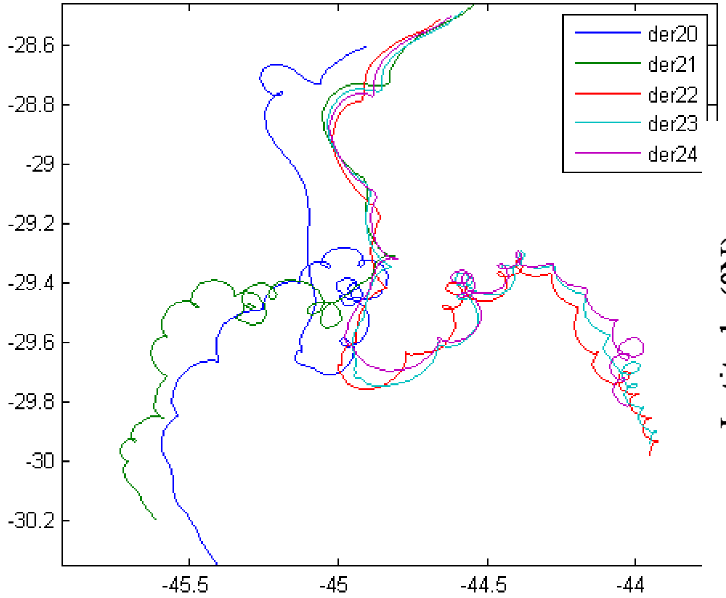

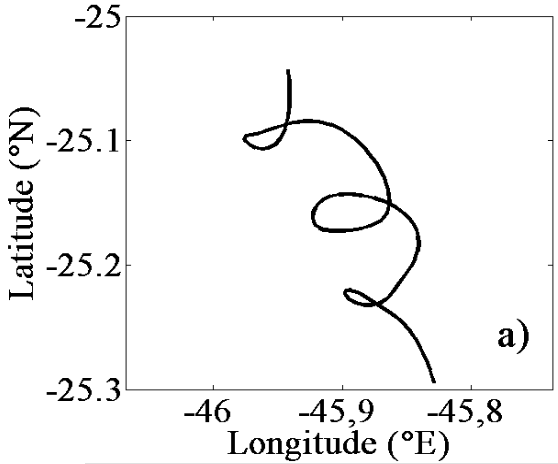

Circular oscillations with Period=2π/f

f is the inertial frequancy

Inertial Period P depends on latitude:

10°N = 69 hours

30°N=24 hours

45°N=16.9 hours

Radius of oscillations: r=U/f

Inertial Oscillations

As friction cannot be completely neglected, inertial oscillations in the real ocean decay in a few days. The amplitude of the inertial motion is proportional to the cumulative wind forcing term and inversely proportional to the water density and thickness of the mixed layer (Park et al, 2005).

Park et al (2005) :

- ✓ inertial amplitudes in the range 0-80 cm/sec with an average value of 13.7 cm/sec.
- ✓ inertial amplitude in the mid-latitude (30-45°N) band exceeds those in both the low (15-30°N) and high (45-60°N) latitude bands
- ✓ In three basins, the amplitude in summer is greater than that in winter by 15%-25%.

Inertial current amplitude from surface drifters. From Chaigneau et al (2008).

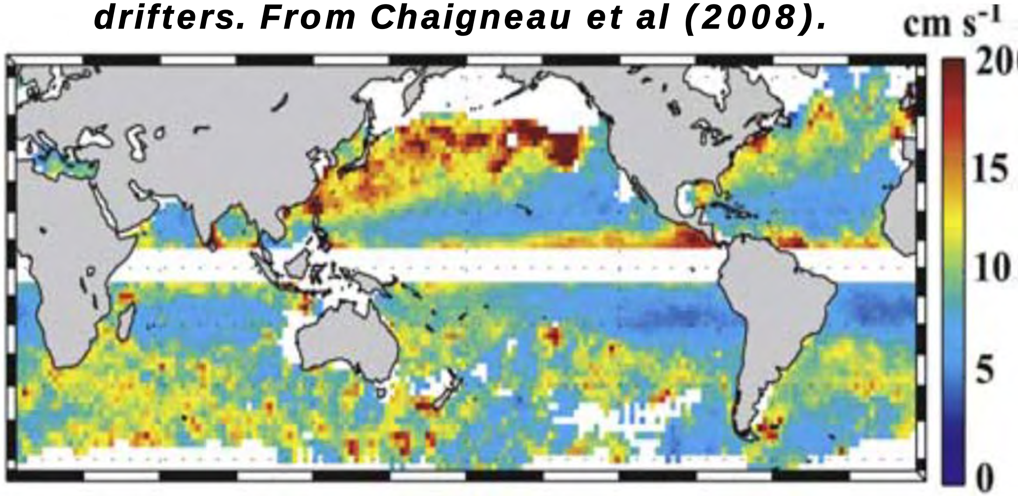

Tidal currents

The ocean tide: Periodic variations of the ocean sea level due to the actions of celestial bodies in rotation around the Earth. More than 400 tidal waves with periods ranging from less than half a day to years.

The vertical motion of the tides near the shore causes the water to move horizontally, creating currents.

Current intensity depends on :

- the different phases of the moon. When the moon is at full or new phases, tidal current velocities are strong. When the moon is at first or third quarter phases, tidal current velocities are weak.
- the relative positions of the moon and Earth. When the moon and Earth are positioned nearest to each other, the currents are stronger than average . When the moon and Earth are at their farthest distance from each other, the currents are weaker .
- the shape of bays and estuaries also can magnify the intensity of tides and the currents they produce

The spatio-temporal scales of the ocean dynamics

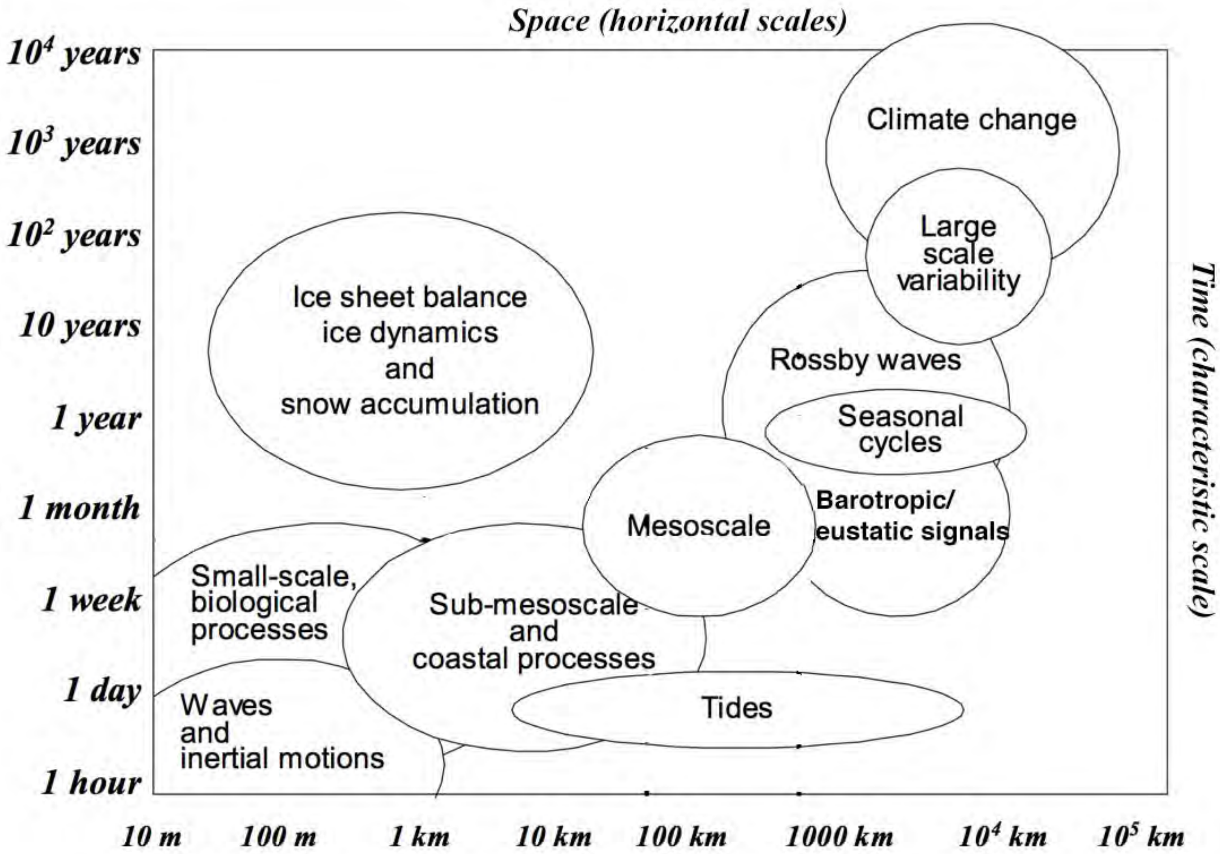

Ocean Circulation monitoring – Observation systems

In-situ measurements

Temperature/salinity profiles -> steric height h_s

$$h_s = -\frac{1}{\rho_0}\int_{-H}^{0} \rho(T,S,z)dz$$

-> baroclinic component of the geostrophic currents

XBT, CTD, gliders, Argo floats

Drifting buoys : Lagrangian measurement of the total ocean current at a given depth

ADCP
Current meters

Eulerian measurement of the current (no stokes drift)

Coastal HF radar

Space measurements

Altimetry

Synthetic Aperture Radar (SAR)

Radiometers/Spectrometers

In-situ measurements: hydrological profiles

XBT (eXpandable BathyThermograph) measure the sea temperature using a thermistor. Depth is inferred from falling rate. Ship of opportunity

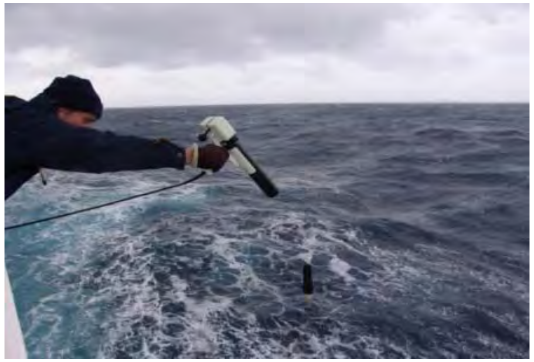

CTD (Conductivity Temperature Depth) Mesure the depth, the temperature and the conductivity (hence the salinity) Oceanographic campaigns

Gliders: The gliders move on a pre-programmed course vertically and horizontally in the water by pumping mineral oil between two bladders, changing the volume of the glider, making it denser or lighter than the surrounding water

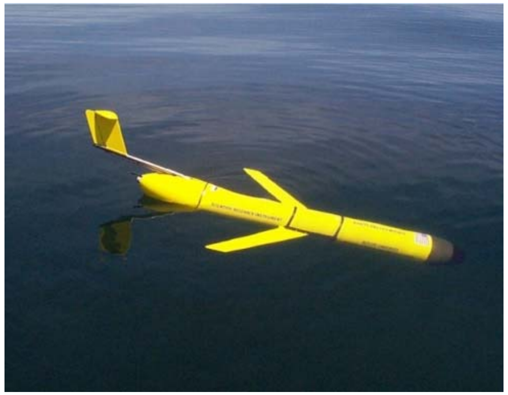

Thermosalinograph measure the sea temperature and salinity

(left) Overall view of the SBE 21 SEACAT Thermosalinograph model. (right) Thermosalinograph installed onboard the NOAA ship Ronald H. Brown.

In-situ measurements: hydrological profiles

Argo profiling floats

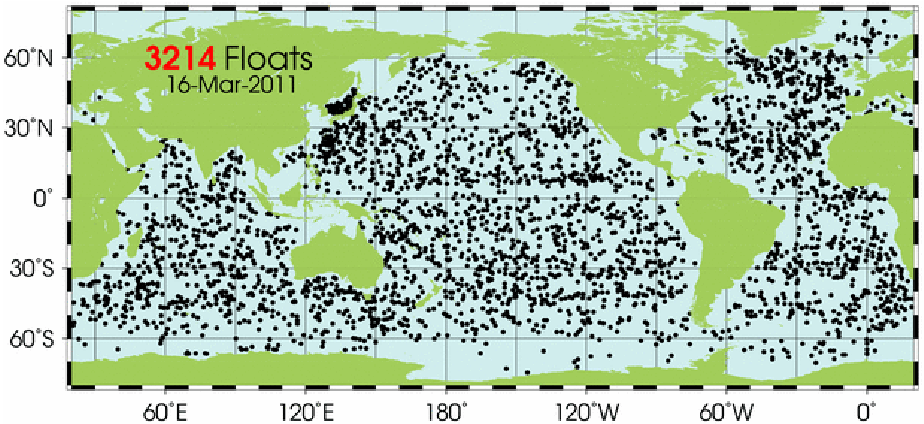

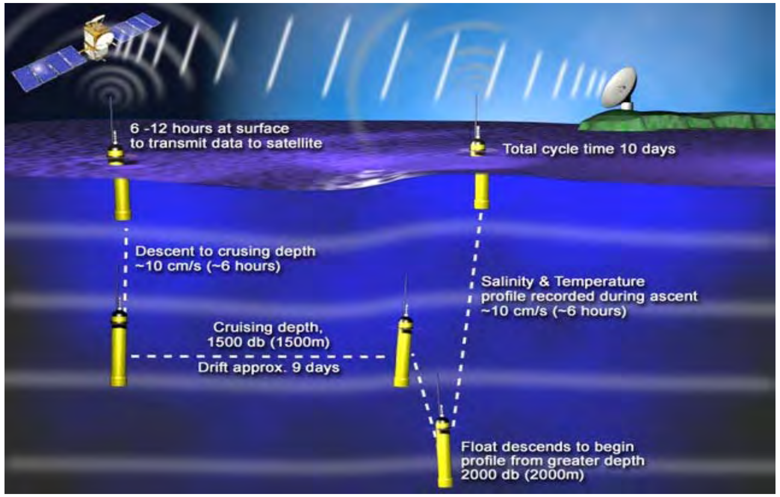

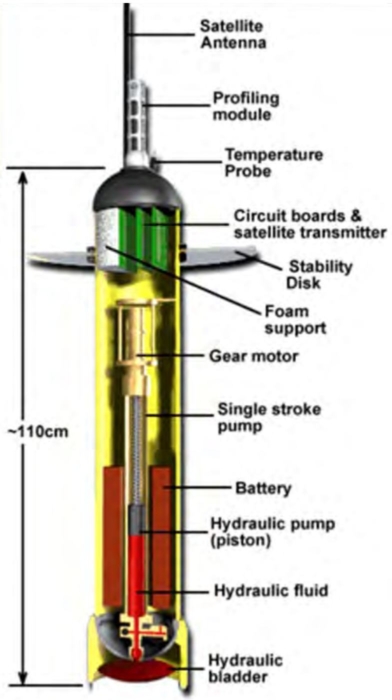

- ❑ Upon deployment floats sink to a pre-specified depth (typically 2,000 meters). They usually remain at this depth for 7-10 days, drifting with the ocean currents. The float will then rise to the ocean surface, where it communicates its data and position to an orbiting satellite. The float then sinks again, continuing the process.
- ❑ A 10 days velocity mean at the parking depth can be deduced from the successive surface positions.
- ❑ Also a surface velocity can be deduced every 10 days from the successive locations of the floats while transmitting its data
- ❑ **Life time** 4 years on average (150 cycles)

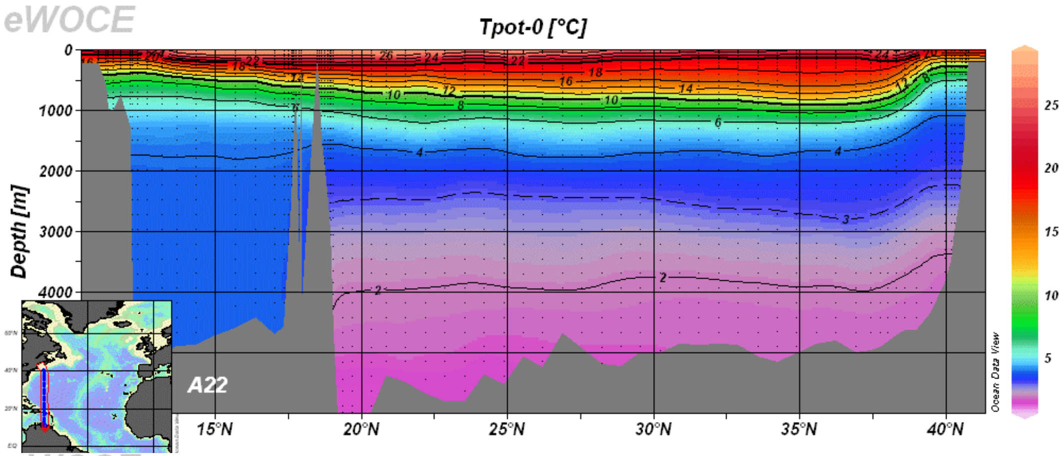

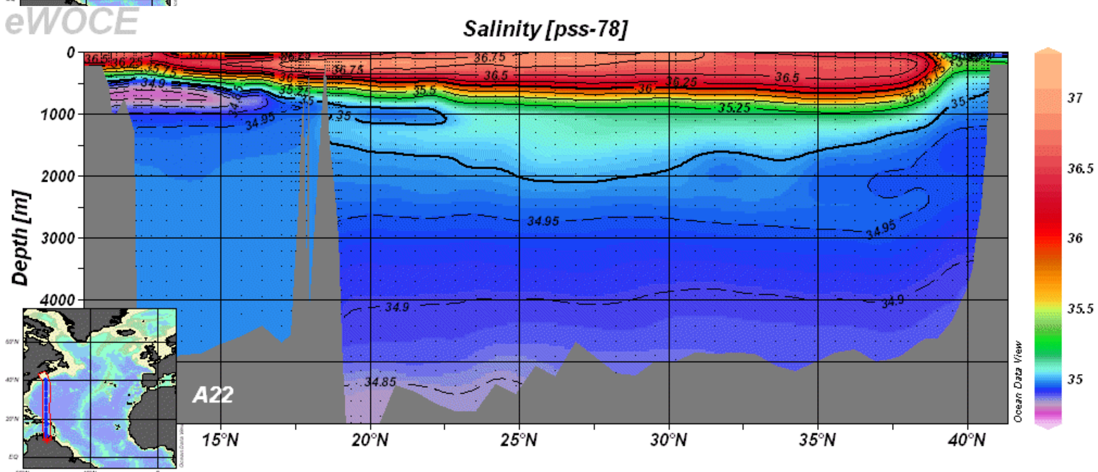

Steric Height

$$h_s = -\frac{1}{\rho_0}\int_{-H}^{0}\rho(T,S,z)dz$$

Baroclinic component of the geostrophic current

$$u_{bc} = -\frac{g}{f}\frac{\partial h}{\partial y} \qquad v_{bc} = \frac{g}{f}\frac{\partial h}{\partial x}$$

mapped absolute velocity at 1000m from T/P–corrected Argo data rel. to Levitus

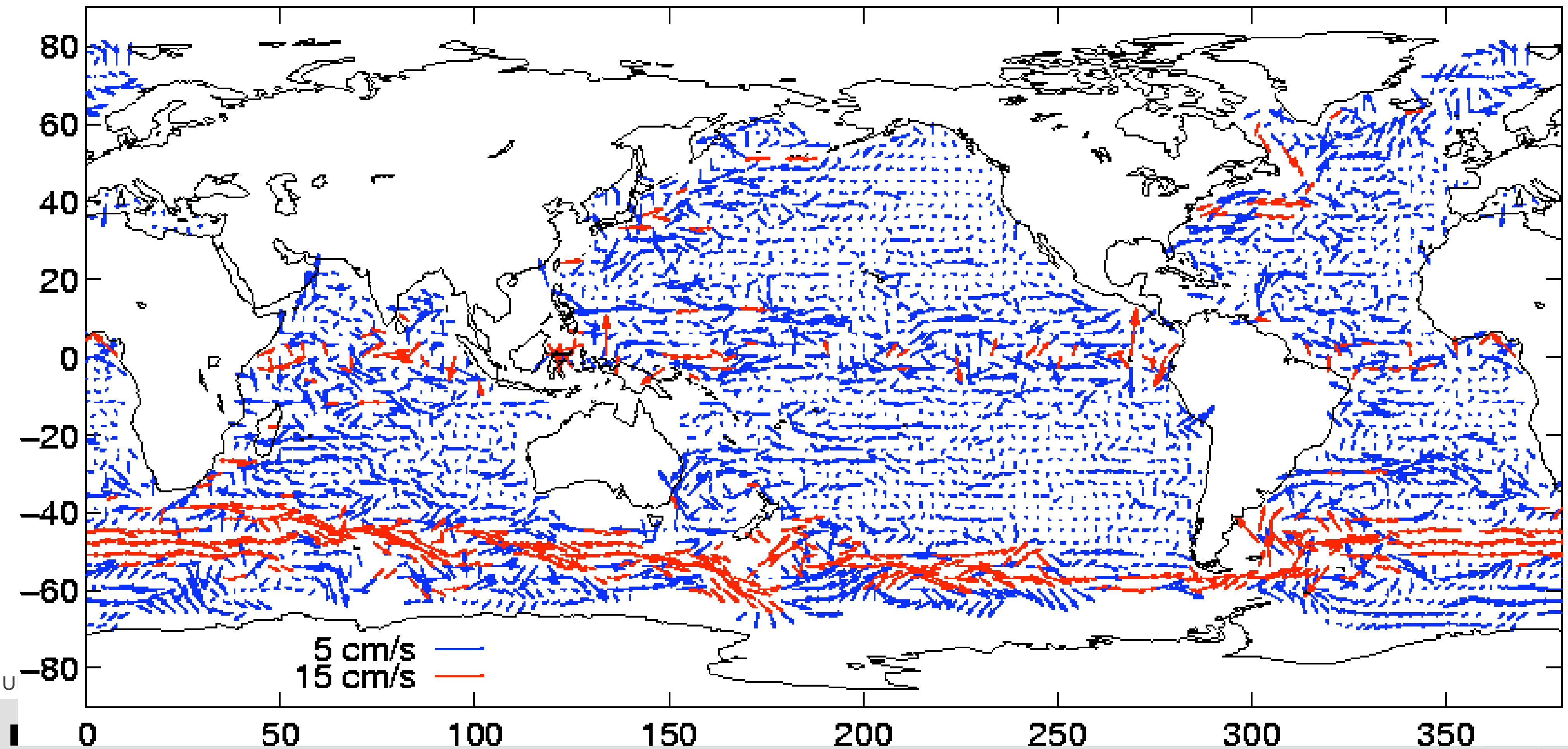

In-Situ measurements: drifting buoys

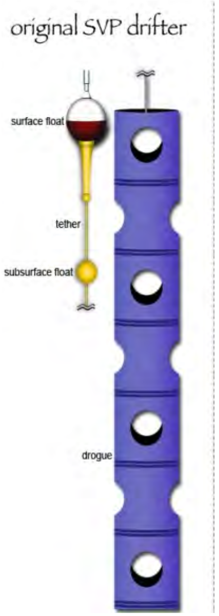

SVP (Surface Velocity Program) type

- Buoy position localized by Argos/Iridium
- Have been designed to minimize the direct wind slippage (less than 0.7 cm/s in 10 m/s winds)
- Holey-Sock drogue centered at 15 m depth -> advected by 15m depth currents
- Drogue loss detection sensor
- After quality control and position processing, regularly sampled velocities are estimated along the buoy trajectory.
- Time sampling: 1 hour, 6 hours
- Life time: ~400 days

Number of obs (1993-2016)

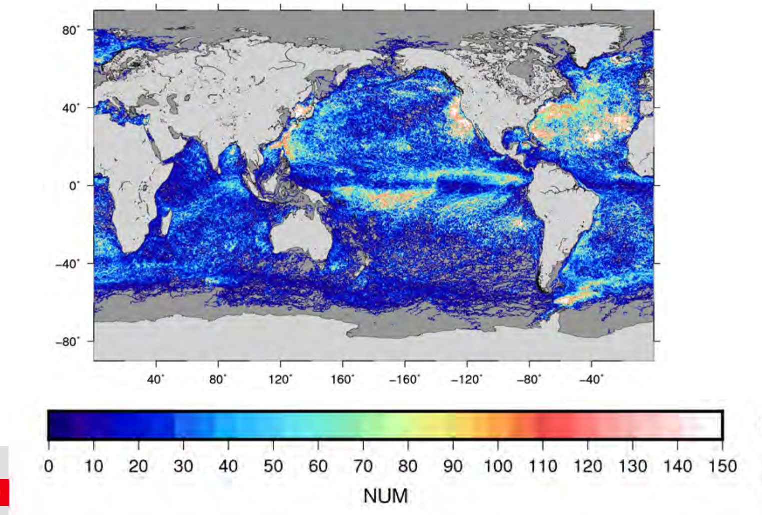

$$U_{buoy} = U_{geost} + U_{ekman} + U_{tides} + U_{inertial} + U_{stokes} + U_{ageost\_hf}$$

In-Situ measurements: drifting buoys

Subsurface drifters - RAFOS

- Mean density adjusted such that the drifter stays at a given depth after immersion.
- A drifting RAFOS float listens and records sound signals from stationary acoustic beacons.
- Programmable life time (<=2 years)
- At the end of its mission, a pre-programmed command releases the float's ballast weight. The float rises to the sea surface and beams the stored acoustic tracking data to two satellites
- After processing the RAFOS trajectory and hence the ocean currents at the RAFOS depth are known at high resolution (several positions per day)

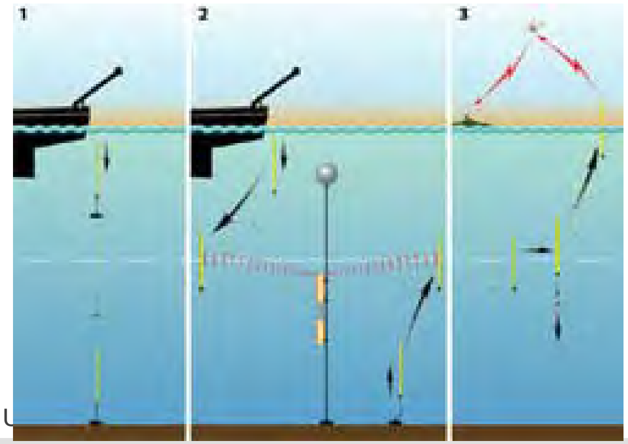

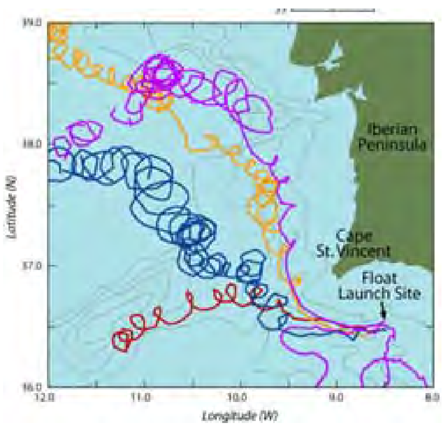

ADCP (Acoustic Doppler Current Profiler)

▪Measure ocean currents speed, direction, depth

▪Uses the Doppler effect: "pings" of sound are transmitted at a constant frequency into the water. As the sound waves travel, they ricochet off particles suspended in the moving water, and reflect back to the instrument. Due to the Doppler effect, sound waves bounced back from a particle moving away from (resp. toward) the profiler have a slightly lowered (higher) frequency when they return. The difference in frequency between the waves the profiler sends out and the waves it receives is called the Doppler shift. The instrument uses this shift to calculate how fast the particle and the water around it are moving.

- placed on the seafloor, attached to a buoy, or mounted on a boat.
- Very high temporal resolution (a few minutes)

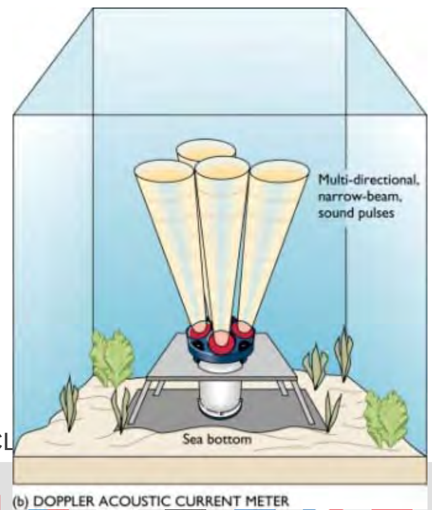

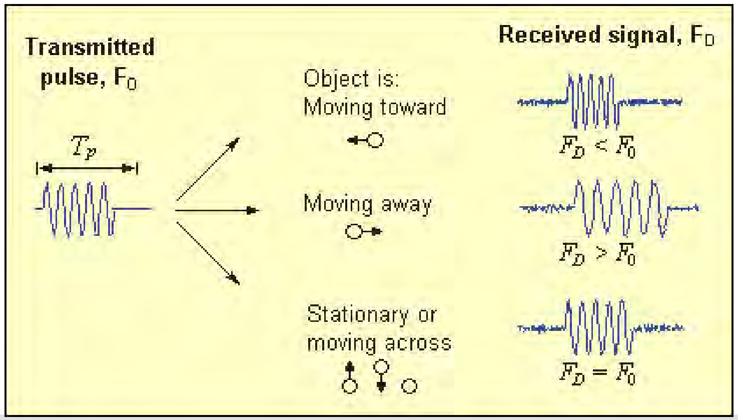

ADCP located offshore Ft. Lauderdale, Florida at a depth of 140 meters

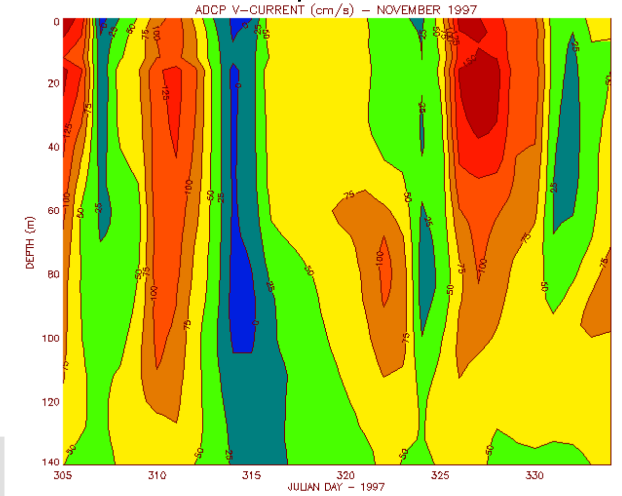

Rotor current meter:
mesures direction and speed of total oceanic currents

A wind vane directs it in the direction of the current and this direction is detected by an internal compass. Speed is measured by a Savenius rotor at the front.

Deployed on moorings

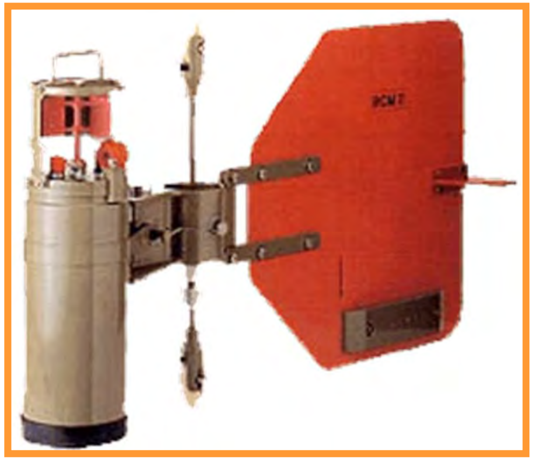

Electromagnetic current meter:
measures the voltage resulting from the motion of a conductor (water flow velocity) through a magnetic field Faraday's law defines the voltage produced in a conductor as the product of the speed of the conductor (water flow velocity) times the magnitude of the magnetic field times the length of the conductor.

In-Situ measurements: HF Radar

HF radar systems use reflections of electromagnetic (EM) waves in the HF radio band (3–30MHz)

- Recorded signal is dominated by EM waves backscattered from ocean surface waves with half the EM wavelength, called Bragg waves, propagating exactly toward or away from the radar.

- In absence of underlying currents (and other surface gravity waves): the backscattered EM waves are Doppler shifted by the linear phase velocity of the Bragg waves $c_0 = \mp\sqrt{\frac{g}{k_B}}$

- In the presence of mean Eulerian currents: the phase velocity differs from c_0 , causing an additional frequency shift df from which the underlying current velocity can be deduced

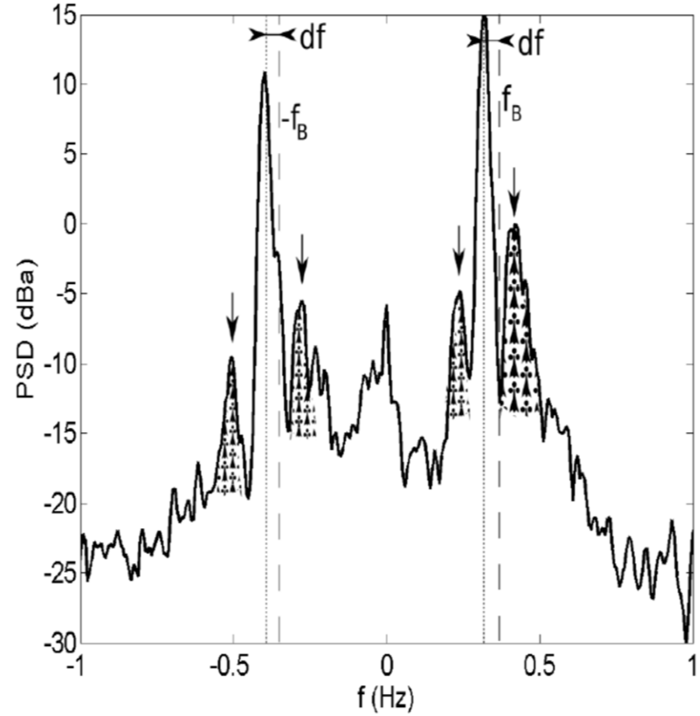

Two prominent peaks due to waves (approaching and receding). Shift from linear wave frequency is due to surface current component in the direction of the antenna

In-Situ measurements: HF Radar

HF radar ocean current systems typically deployed along the coast. Two radars are needed to estimate the 2 components velocity vector. The measurements provide synoptic current maps over a few to several thousand square kilometers of the ocean surface at high spatio-temporal resolution (<1 hour, 5-20 kilometers)

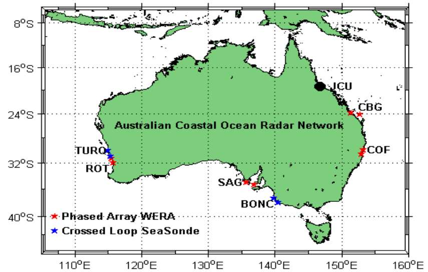

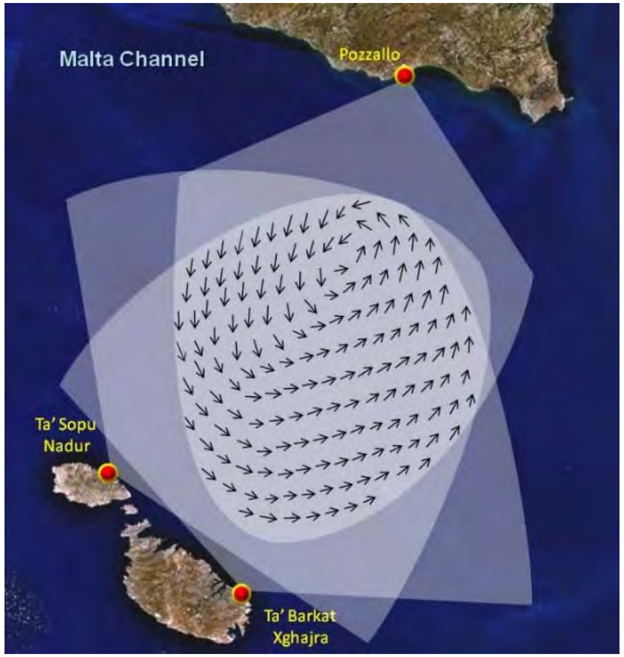

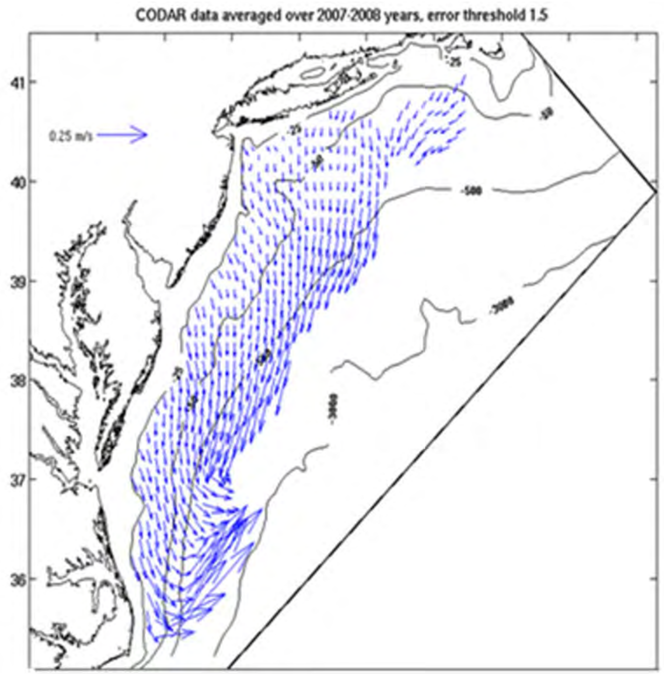

In-Situ measurements: HF Radar

There has been some controversy about the ability of HF surface radar to measure Stokes drift.
Many recent research projects were conducted with the assumption that Stokes drift is present in the HF radar surface current data (Graber and Haus 1997; Gremes-Cordero et al. 2003; Ullman et al. 2006).
On the contrary, Rohrs et al (2015) compared HF radar velocities to ADCP velocity measurements on one hand (Eulerian velocity measurement) and surface drifters on the other hand (Lagrangian velocity measurements) and concluded that HF radars do not measure the stokes drift.

Recent review by Chavanne et al, 2018: « In conclusion, a definitive answer to the question of whether HF radars measure the surface Stokes drift, or a related quantity, will require further experimental investigations”

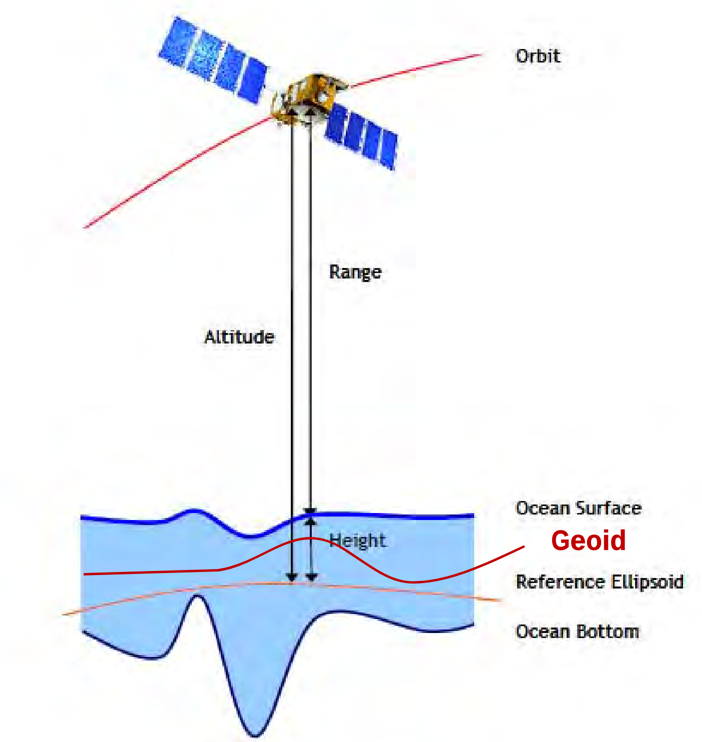

Altitude-Range = η = G + h

Accurately measured by altimeter

Geoid

Ocean dynamic topography

The repeat-track method

$$\overline{\eta}_P = G + \overline{h}_P$$

$$\eta' = \eta - \overline{\eta}_P = \mathbf{h}'$$

Sea Level Anomalies (SLA)

High along-track resolution (300m / 7km)

Space measurements: Altimetry

Altimetric anomalies along the tracks from 4 different satellites in the Gulfstream.

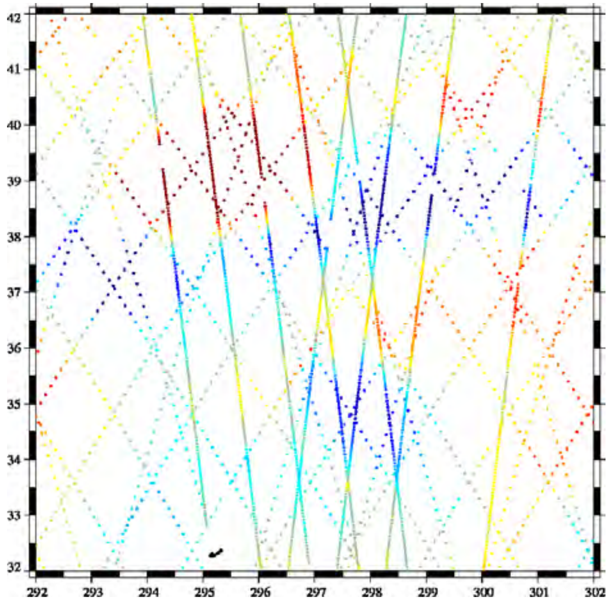

Objective Analysis

$$\theta_{est}(\mathrm{x}) = \sum_{i=1}^{n} \sum_{j=1}^{n} A_{ij}^{-1} C_{xj} \Phi_{obs^{i}}$$

Altimeter anomaly map

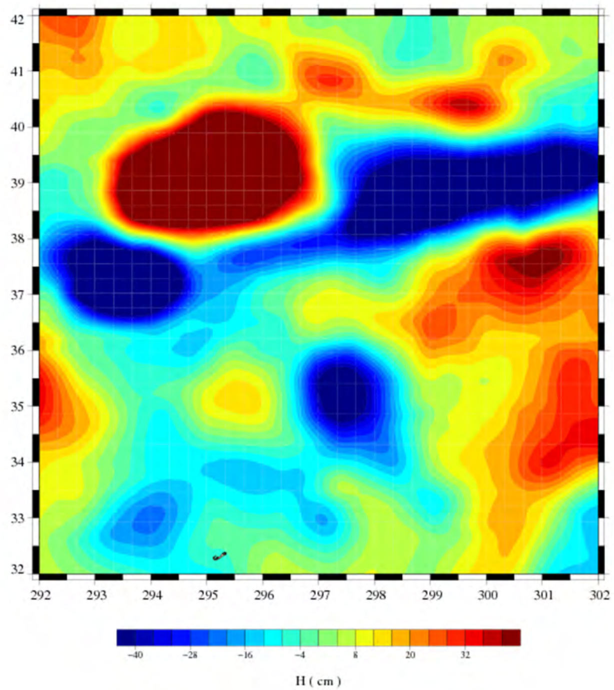

$$A_{ij} = \left\langle \Phi_{obs^{i}} \Phi_{obs^{j}} \right\rangle = \left\langle \Phi_i \Phi_j \right\rangle + \left\langle \varepsilon_i \varepsilon_j \right\rangle$$

$$C_{xi} = \left\langle \theta(x)\, \Phi_{obs^{i}} \right\rangle = \left\langle \theta(x)\, \Phi_i \right\rangle$$

Space measurements: Altimetry   System resolution

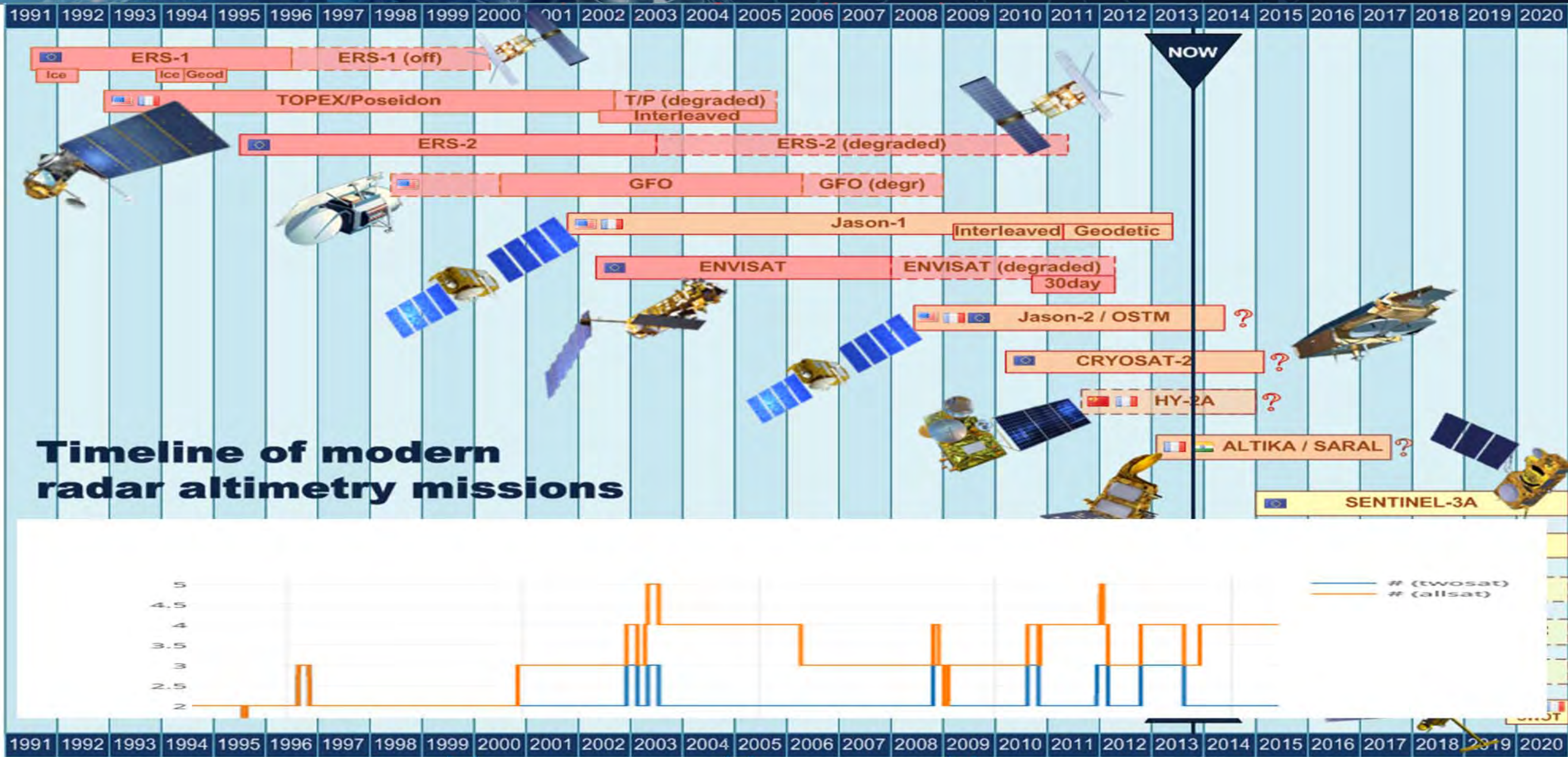

Spatial resolution achieved for a 10 days temporal resolution

2 satellites
250-300km

4 satellites
100 km

3 satellites
150 km

From Sea Level Anomaly to the Absolute Dynamic Topography

Altimetric Anomaly (SLA)

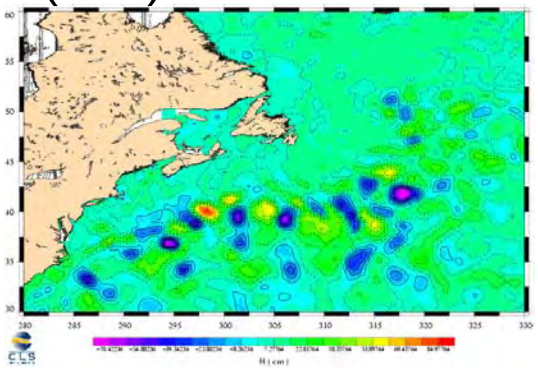

\+ Mean Dynamic Topography

Tomorrow's lecture

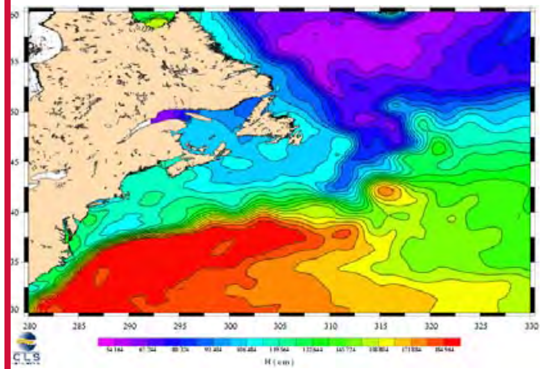

= Absolute Dynamic Topography

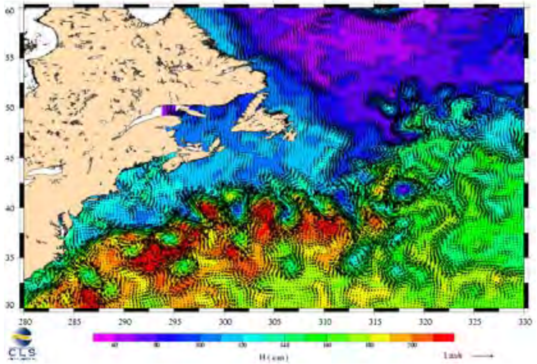

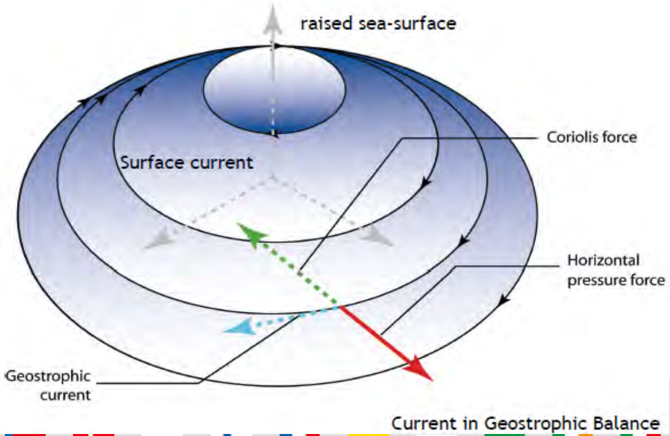

$$u_g = -\frac{g}{f}\frac{\partial h}{\partial y}$$

$$v_g = \frac{g}{f}\frac{\partial h}{\partial x}$$

Geostrophic approximation

Space measurements: SAR Doppler

Chapron et al, 2005 ; Johannessen et al, 2008; Rouault et al, 2010 have demonstrated the strong value of using the Doppler shift measurements from the ENVISAT ASAR data for retrieving the radial component of the surface current at 4-8 km resolution every 2-3 days.

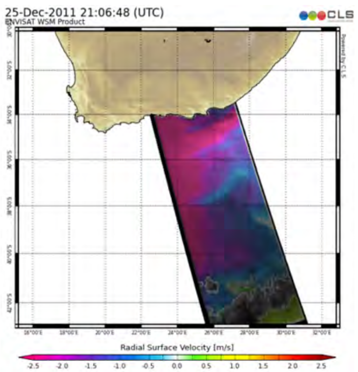

A Doppler shift is measured between the Signal emitted by the instrument and the signal **backscattered** by the sea surface and **measured** by the SAR antenna. It is due to:

- The known movement of the satellite in orbit,
- A wave-state contribution highly correlated to wind speed which can be estimated using an empirical relationship between the range Doppler velocity and the near surface wind field, Mouche et al. (2012) with a C-band Doppler (CDOP) algorithm. These local wind contributions are mainly **from wave orbital motion, but also from Ekman and Stokes drift.**

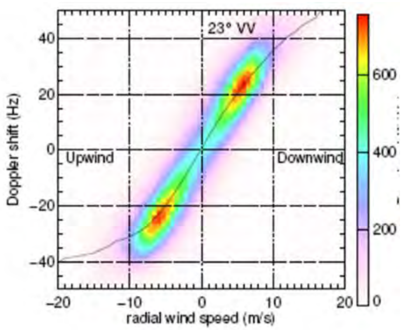

-a **measure of the sea surface current**, with 10km pixel size that contains the contributions, projected onto the range direction, of the **geostrophic currents, the tidal currents, the inertial oscillations**.

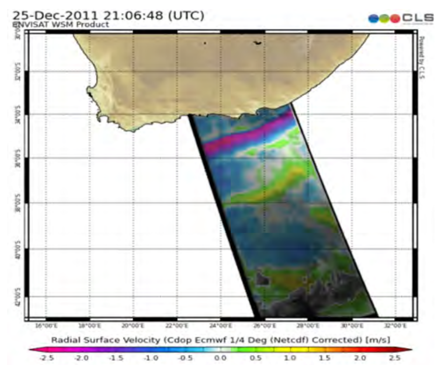

Future satellite mission concepts for direct current measurement using Doppler

Different concepts with a common strategy:

- ❑ Delayed Doppler effect is used to infer the sea motion in the satellite range direction
- ❑ Each scene is viewed from 2 or more azimuth angle to get motion vector

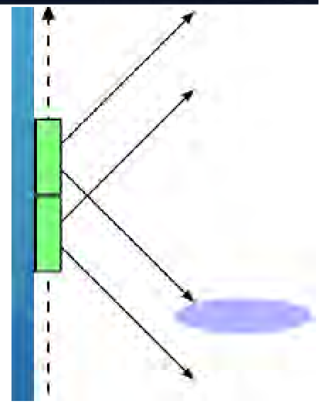

SEASTAR: Squinted Along-track interferometric SAR:
two-dimensional maps of total ocean surface current vectors and wind vectors at 1km resolution with unprecedented accuracy, supported by coincident directional swell spectra in coastal, shelves and polar seas.

DOPSCAT (EU) / WaCM (Wind and Current Mission, US): : scatterometry with Doppler capability to provide simultaneous measurements of marine winds and surface currents. The mission seeks to monitor global surface ocean currents on a daily basis with a spatial resolution around 25km and errors better than 0.1-0.2 m/s

SKIM (Sea surface Kinematics Multiscale monitoring – EE9 candidate):
Doppler-enabled rotating near-nadir Ka-band altimeter to measure total surface current vectors with an accuracy of 0.1 m/s for 40km / 10 days resolution together with the full directional wave spectrum.

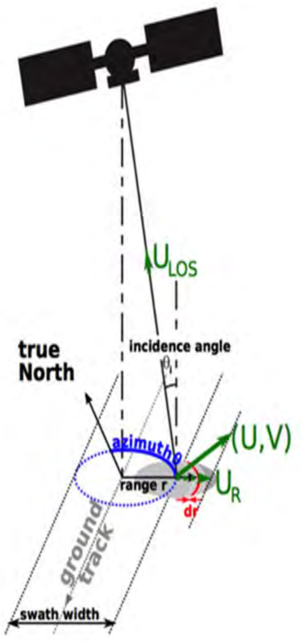

Other space measurements related to ocean circulation

- Passive radiometers

Measure the spectral signature of
The sun radiation reflected at the
surface of the ocean
-> Ocean colour

The energy emitted by the
surface of the ocean
-> Temperature, Salinity

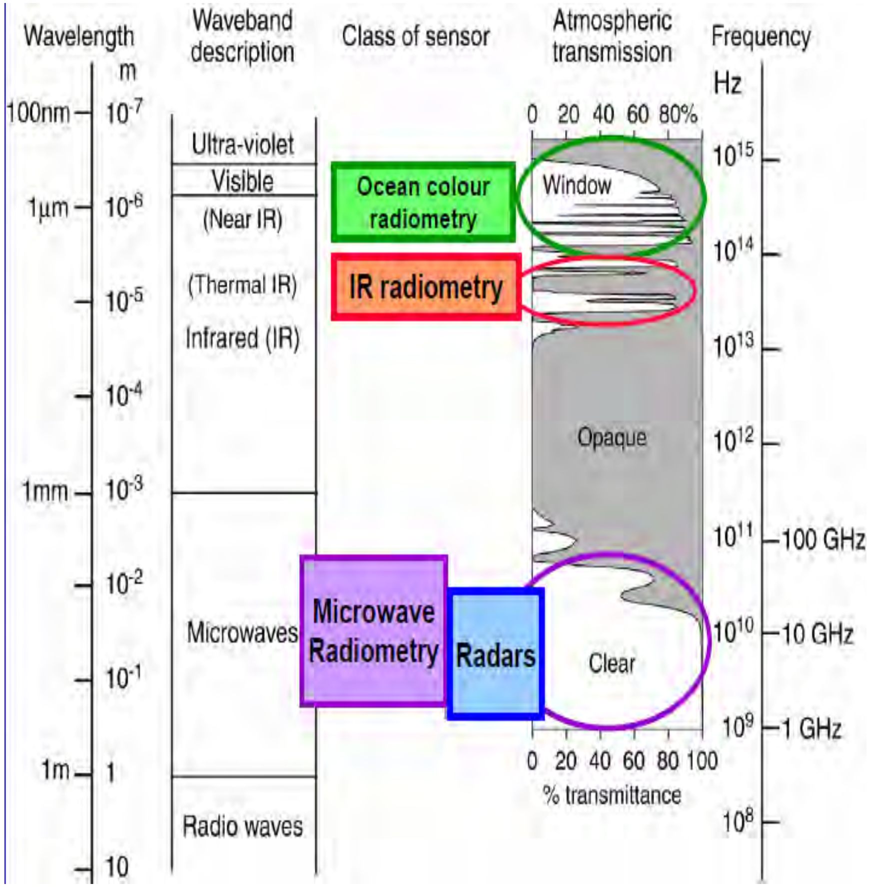

Other space measurements related to ocean circulation

January, 1st 2004
Microwave SST product
Altimeter geostrophic velocities

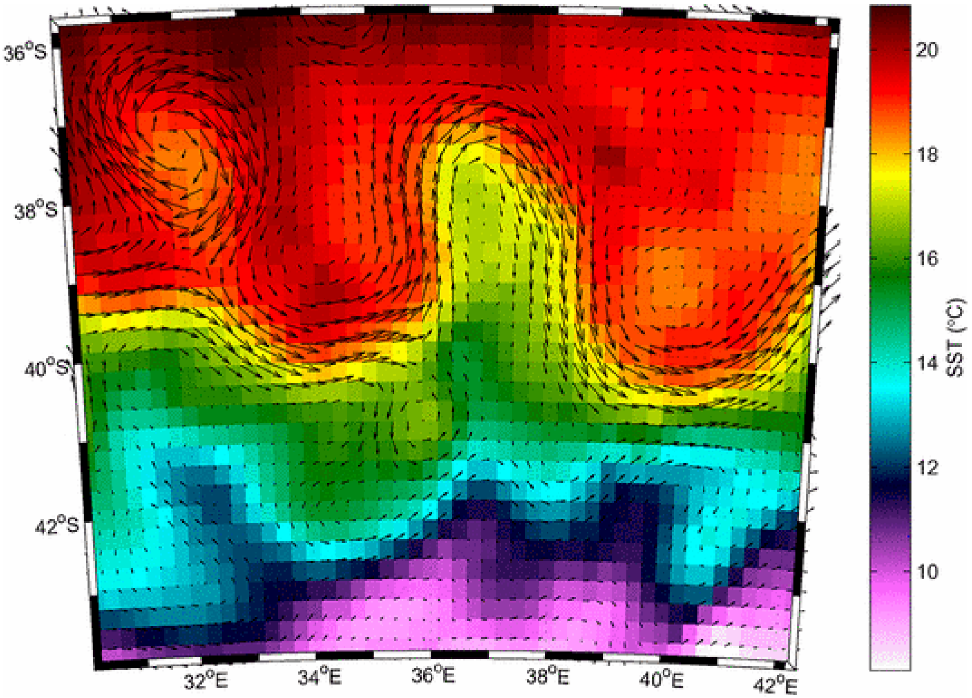

❖ OC (under certain circumstances), SST, salinity can be considered as passive tracers advected by the ocean currents.

-> the analysis of successive images informs on the ocean current field ***MCC, optical flow***

❖ Under favourable environmental conditions, the streamfunction ψ from which geostrophic velocities are derived, can be calculated from surface density values from which SST may be considered as a proxy ***e-SQG approximation***

The Maximum Cross Correlation (MCC) method

The method consists in calculating the displacement of small regions of patterns from one image to another.
We look for the pair δx_{max} δy_{max} that achieves the maximum cross-correlation between a target region in the first image and a candidate region in the second image

$$[u\ v] = [\delta x_{max}\ \delta y_{max}\ ] / \Delta t$$

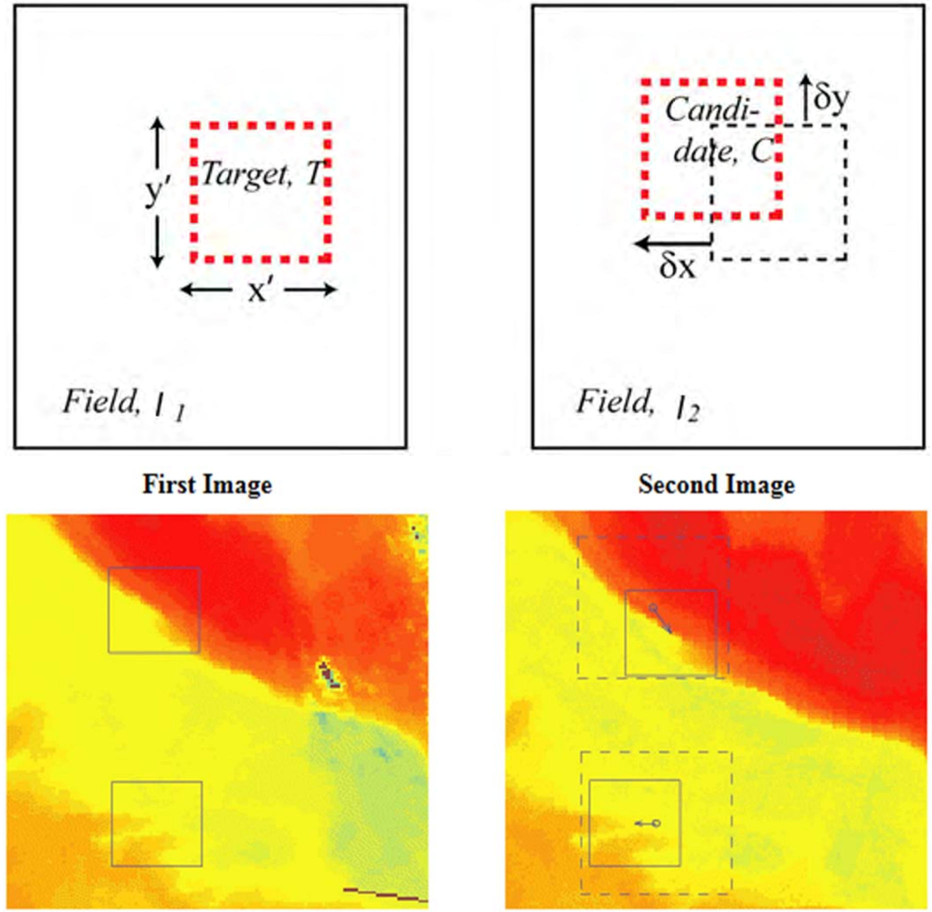

This can be applied on any image: a brightness temperature, a water-leaving radiance or a derived product such as sea surface temperature (SST) or chlorophyll concentration

Emery et al, 1986

Application on GOCI (Geostationnary Ocean Color Imager) Ocean Color images in the Tsushima Strait

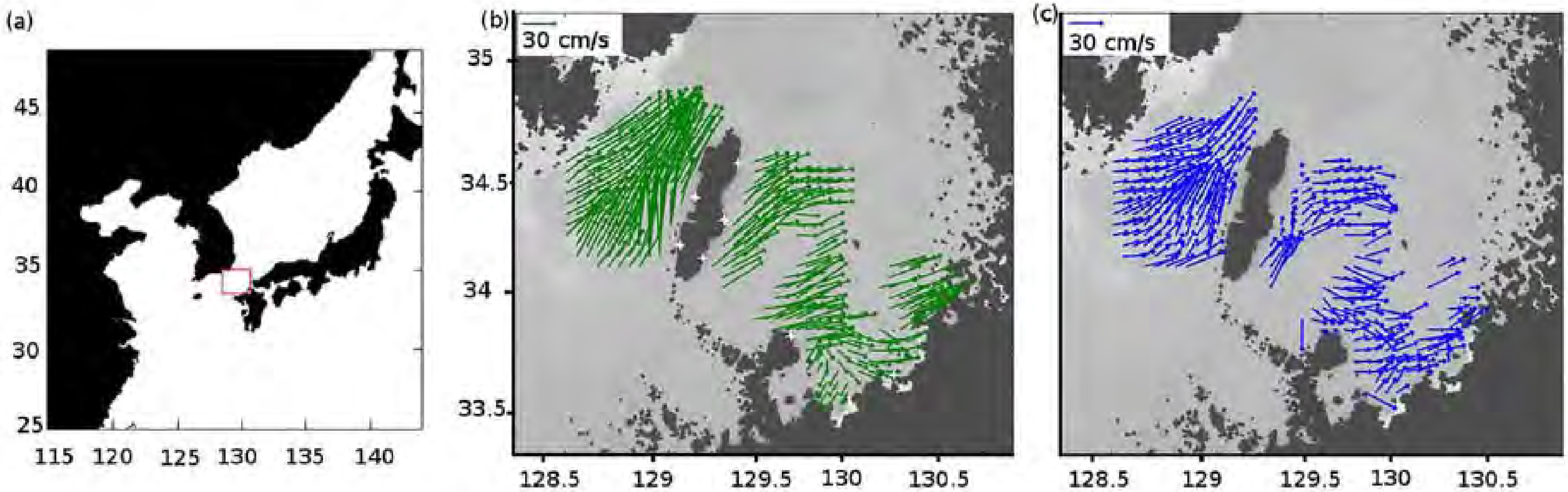

Figure 2. (a) Total region covered by the GOCI sensor with the red box indicating the Tsushima Strait area used in this study; (b) arrows indicate mean velocities from HF radar and locations of the 7 HF radar stations are shown as white dots; c) arrows indicate mean velocities from MCC methodology. Data are from 26 March 2012 and all MCC image pairs have been used. Velocities are the mean over corresponding time periods and locations. Radar-derived velocities are only shown where there are MCC velocities.

Warren et al, 2016

The Maximum Cross Correlation (MCC) method

Limitations

- **Cloud-cover and isothermal/isochromatic ocean surface conditions drastically limit the spatial and temporal velocity coverage provided by the MCC method**. Clouds block the ocean surface in both thermal and ocean color imagery, and there are no features for the MCC method to track in isothermal/isochromatic regions.
- Accurate spatial alignment and coregistration of the imagery used in feature tracking is required. Consequently, the technique has been more **often used in coastal regions**, where landmarks are available to renavigate the satellite data.
- MCC techniques work well for intervals between images of 6-24 hrs, but are not so reliable for longer gaps due to evolution of the features, including rotation and shear.

Effective Surface Quasi Geostrophy (E-SQG) Method

Under favourable environmental conditions, the streamfunction h from which geostrophic velocities are derived, can be calculated from surface density values:

Lapeyre et al, 2006; Klein et al., 2008

Inversion of the Quasi Geostrophic Potentiel Vorticity conservation equation in the horizontal Fourier transform domain (valid for space scales of 10-200km)

$$\begin{cases} \frac{\partial}{\partial y} h_{sqg} = -u \\ \frac{\partial}{\partial x} h_{sqg} = v \end{cases} \Leftarrow \hat{h}_{sqg}(\vec{k}, z) = \frac{f}{N_{eff}\,\rho_0 k}\,\hat{\rho}'_s(\vec{k}) \cdot e^{\left(\frac{N_{eff}\,kz}{f_0}\right)} \Rightarrow \rho'_s = -\alpha \cdot T_s' - \beta S_s' = -\alpha' T_s'$$

Currents Streamfunction Surface Density Anomalies **SST anomaly**

N_{eff} is the effective Brunt-Vaisala frequency (constant stratification assumed)

$\alpha' N_{eff}^{-1}$ is a free parameter that needs to be set up to account both interior PV and the partial compensation of salinity and temperature.

SYNERGY: This can be done by using the information about the energy spectrum provided by altimeters [Isern Fontanet et al, 2006; *Haro and Fontanet, 2013]. See tomorrow's lecture*

Effective Surface Quasi Geostrophy (E-SQG) Method

Limitations

- The coldest SST anomalies are reported to efficiently trace the lowest SSH anomalies for all seasons, while the warmest SST anomalies solely match the largest SSH anomalies during winter.
- SST-derived SSH reconstruction using the surface quasi geostrophic approximation should take into account stratification effects, especially during summer

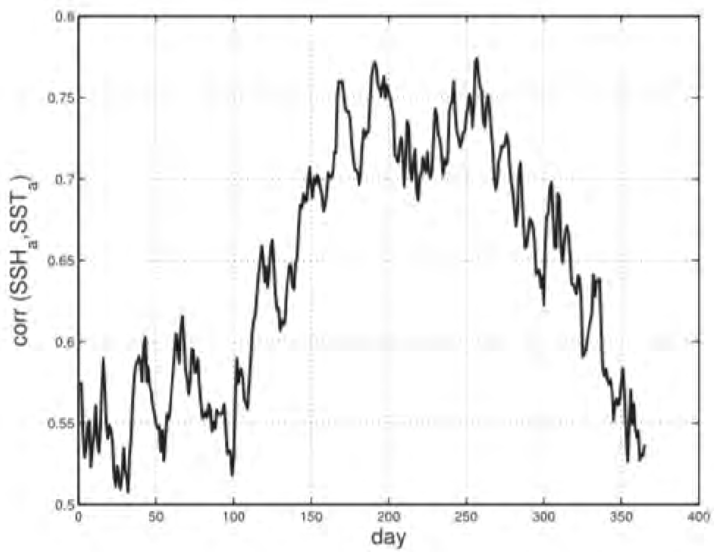

Time series of the global correlation between SSH and SST anomaly fields in 2004 in the Agulhas return current

Legoff et al, 2016

« Optical flow » methods: inversion of a tracer conservation equation

Require the velocity field (u,v) to obey the tracer concentration c evolution equation and inverse it for the velocity vector:

$$\frac{\partial c}{\partial t} + u\frac{\partial c}{\partial x} + v\frac{\partial c}{\partial y} = F(x,y,t)$$

c represents the concentration of any tracer as Sea Surface Temperature, Sea Surface Salinity, Chl-a concentration,

F(x,y,t) represents the source and sink terms

Limitation: only **along-gradient velocity** information can be retrieved from the tracer distribution at subsequent times in **strong gradients areas**. **+ strong uncertainties on F**

Synergy : The method is used on successive SST images using the altimeter geostrophic velocities as background so as to obtain an optimized 'blended' velocity (u_{opt}, v_{opt}). *Rio et al, 2016* - ***see tomorrow's lecture***

CONCLUSION

Observing system	Coverage	Spatial resolution	Temporal resolution	Current component measured
Hydrological profiles (XBT, CTD, gliders, Argo floats	Surface and depth sparse	Vert. 1 m	Yoyo: 20 minutes	Baroclinic component of the geostrophic current
Drifting buoys	Surface and depth sparse	Along-track	Surf: 1 hour/ 6 hours Deep: 1 day	Total current
ADCP	Surface and depth sparse	Vert. 10 m	1 hour	Total current
Current meters	Surface and depth sparse		30 minutes	Total current
HF radar	Surface costal	5-20 km	< 1 hour	Total (?) current
Altimeter	surface Global	Grid: 100 km	Grid: 10 days	Geostrophic current
SAR	Super sites	4-8 km	2-3 days	Radial component of total current minus wind drift
SST	MW: global IR: cloud sensitive	25 km 10 km	1 day	SQG: geostrophic MCC/OF: total / radial current in strong gradient areas

Complementarity of space and in-situ observations

No observing system actually provides global, high spatio-temporal resolution measurements of the ocean circulation needed for a routine, global monitoring

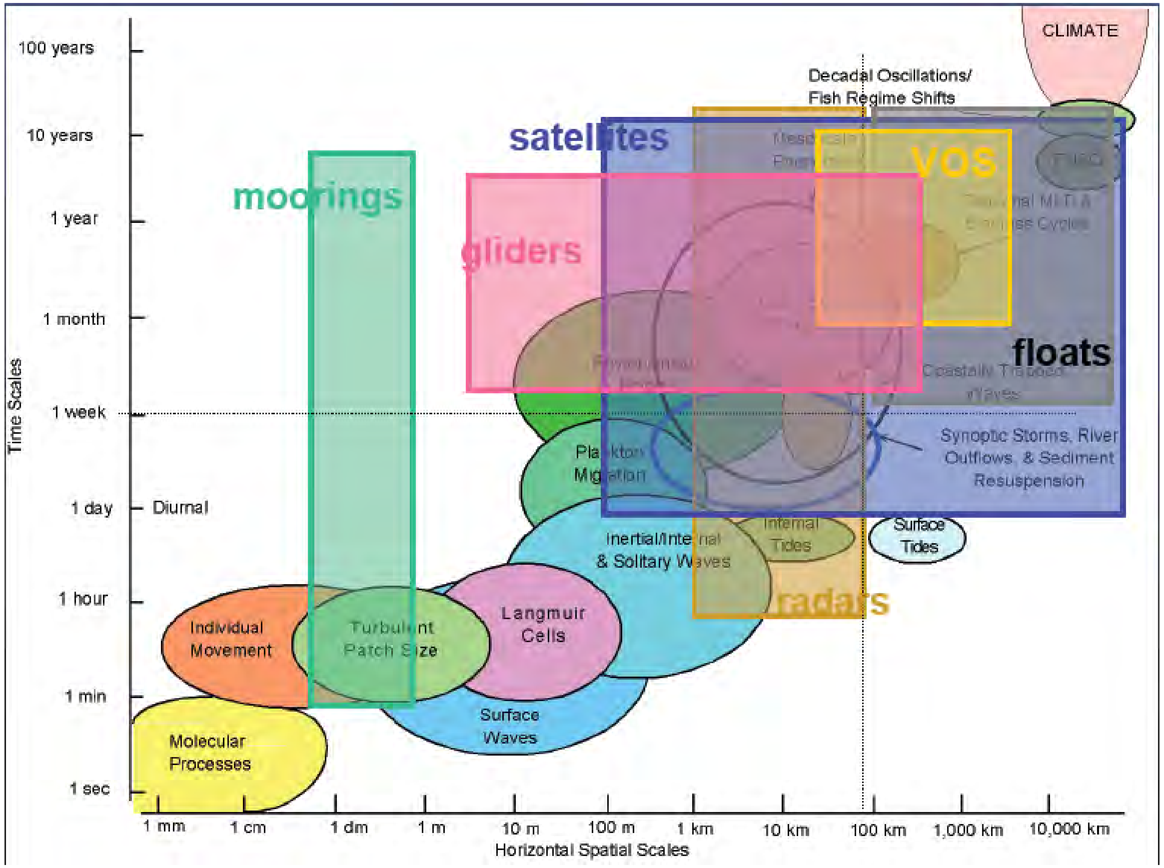

Synergy is needed : See you Tomorrow!